



AEOLIAN TRANSPORT OVER A FLAT SEDIMENT SURFACE
by Leo C. van Rijn; www.leovanrijn-sediment.com

- 1. Introduction**
- 2. Modes of wind-blown particle transport**
- 3. Physics of sand transport by wind**
 - 3.1 Processes**
 - 3.2 Initiation of saltation**
 - 3.3 Saltation characteristics**
 - 3.4 Modification of near-surface wind velocity profile**
 - 3.5 Saltation to steady state**
 - 3.6 Saltation mass flux in saturated conditions**
 - 3.7 Processes affecting sediment transport**
- 4. Wind-blown sand transport on beaches**
- 5. Preventive measures to reduce erosion**
- 6. References**



1. Introduction

The wind-driven emission, transport, and deposition processes of sand and dust by wind are termed aeolian processes, after the Greek god Aeolus, the keeper of the winds. Aeolian processes occur wherever there is a supply of granular material and atmospheric winds of sufficient strength: in deserts, on beaches, and in other sparsely vegetated areas, such as dry lake beds. The blowing of sand and dust in these regions helps to shape the surface through the formation of sand dunes and ripples.

The terms dust and sand usually refer to solid particles that are created from the weathering of rocks. Sand is defined as mineral particles with diameters between 63 and 2,000 μm , whereas dust is defined as particles with diameters smaller than 63 μm .

Aeolian sand transport depends on:

- windspeed, direction and duration,
- sand composition (particle size and distribution),
- environmental conditions (moisture, vegetation, beach width, dune height, beach nourishment practices, type of coast: erosive, stabile or accretive).

Many descriptions of the present note are taken from the work of De Kok et al. 2012.

The file AEOLIANTRANSPORT.xls is used for computations.

2. Modes of wind-blown particle transport

The transport of particles by wind can occur in several modes, which depend predominantly on particle size and wind speed. As wind speed increases, sand particles of about 100 μm diameter are the first to be moved by fluid drag. After lifting, these particles hop along the surface in a process known as saltation. The impact of these saltators on the soil surface can mobilize particles of a wide range of sizes. Very small particles are predominantly ejected from the soil by the impacts of saltating particles. Following ejection, dust particles are susceptible to turbulent fluctuations and thus usually enter short-term or long-term suspension.

The impacts of saltating particles can also mobilize other particles. However, the acceleration of particles with diameters in excess of about 500 μm is strongly limited by their large inertia, and these particles generally do not saltate. Instead, they usually settle back to the soil after a short hop (< 10 mm) in a mode of transport known as reptation. Alternatively, larger particles can roll or slide along the surface, driven by impacts of saltating particles and wind drag forces in a mode of transport known as creep. Creep and reptation can account for a substantial fraction of the total wind-blown sand flux.

The transport of particles by wind can be crudely separated into several physical regimes (**Figure 2.1**):

- long-term suspension (< 20 μm),
- short-term suspension (20 – 63 μm),
- saltation (63 – 500 μm), and
- reptation and creep (> 500 μm).

Furthermore, we can distinguish between:

- transport-limited saltation, for which the amount of saltating sand is limited by the availability of wind momentum to transport the sand;
- supply-limited saltation, for which the amount of saltating sand is limited by the availability of loose soil particles that can participate in saltation, which can occur for crusted or wet soils.

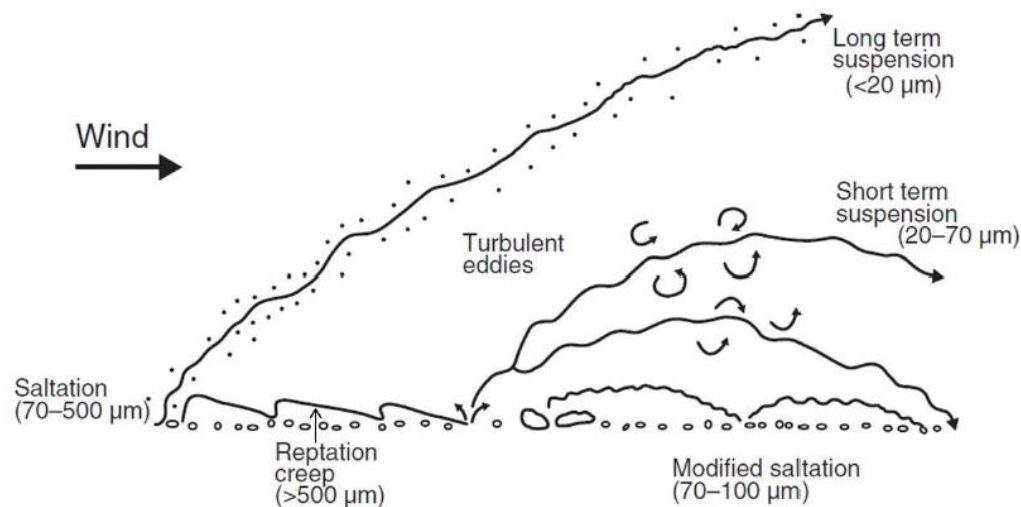


Figure 2.1 Modes of wind-blown transport of sediment (De Kok et al., 2012)

3. Physics of sand transport by wind

3.1 Processes

Saltation plays a central role in aeolian processes. Saltation is initiated when the wind stress is sufficient to lift surface particles into the wind stream, which for loose sand occurs around a wind speed of 4 to 6 m/s. Following initiation, the lifted particles are accelerated by wind into ballistic trajectories and the resulting impacts on the soil bed can eject, or splash, new saltating particles into the wind stream. This process produces an exponential increase in the particle concentration, which leads to increasing drag on the wind, thereby retarding the wind speed in the saltation layer. It is this slowing of the wind that acts as a negative feedback by reducing particle speeds, and thus the splashing of new particles into saltation, which ultimately limits the number of saltating particles and thereby partially determines the characteristics of steady state saltation.

The physics of aeolian saltation can be roughly divided into four main physical processes:

- the initiation of saltation by the aerodynamic lifting of surface particles,
- the subsequent trajectories of saltating particles,
- the splashing of surface particles into saltation by impacting saltators, and
- the modification of the wind profile by the drag of saltating particles.

3.2 Initiation of saltation

Saltation is initiated by the lifting of a small number of particles by wind stress.

The value of the wind stress at which this occurs is termed the fluid or static threshold. This threshold depends not only on the properties of the fluid, but also on the gravitational and interparticle cohesion forces that oppose the fluid lifting.

The fluid threshold is distinct from the dynamic or impact threshold, which is the lowest wind stress at which saltation can be sustained after it has been initiated. The impact threshold is smaller than the fluid threshold because the transfer of momentum to the surface through particle impacts is more efficient than through drag.



An expression for the fluid threshold can be derived from the force balance of a stationary surface particle: yielding (see **Figure 3.1**):

$$u_{*,cr} = \alpha_{cr} \alpha_{mois} [(\rho_s/\rho_{air} - 1)g d]^{0.5} \quad (3.1)$$

$$U_{wind,cr} = (u_{*,cr}/\kappa)/\ln(30h_{wind}/k_s) \quad (3.2)$$

Bagnold (1941) found $\alpha_{cr} \approx 0.11$ for dry loose sand $> 63 \mu\text{m}$.

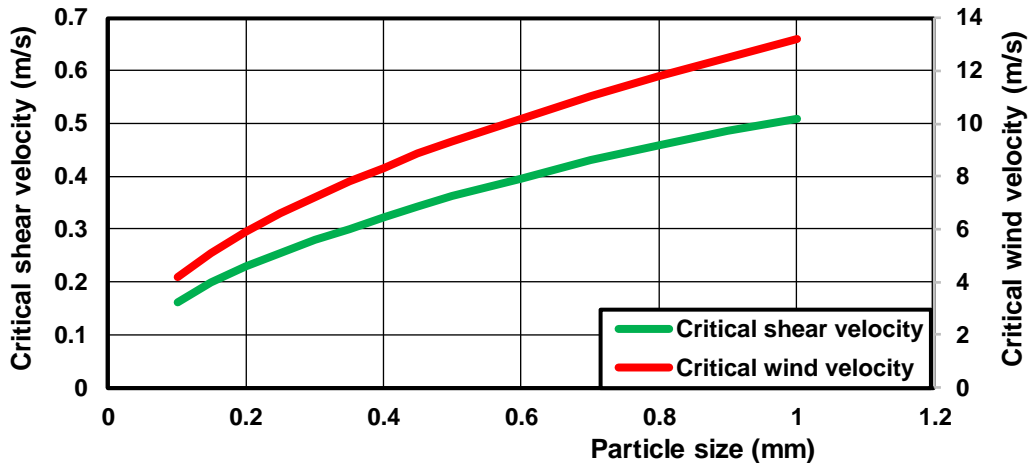


Figure 3.1 Critical shear velocity and critical wind velocity of dry, loose sand particles ($k_s = 0.01 \text{ m}$, $h_{wind} = 10 \text{ m}$, $\kappa = 0.4$, $\rho_{air} = 1.2 \text{ kg/m}^3$)

3.3 Saltation characteristics

After saltation has been initiated, lifted sand particles undergo ballistic trajectories that are determined primarily by the gravitational and aerodynamic drag forces. The acceleration of particles by the drag force transfers momentum from the fluid to the saltating particles and thus retards the wind profile in the saltation layer.

Numerical computer simulations shows saltation heights of 15 to 30 mm and saltation lengths of 200 to 500 mm for particles in the range of 100 to 500 μm under a wind speed of about 10 m/s ($u_* \approx 0.4 \text{ m/s}$). Saltation heights are about 50 mm for a wind speed of 25 m/s.

The ballistic trajectories of saltating particles are terminated by a collision with the surface. These particle impacts onto the soil surface are a critical process in saltation for two reasons. First, the splashing of surface particles by impacting particles is the main source of new saltators after saltation has been initiated. And second, since particles strike the soil nearly horizontally and rebound at angles of about 40° from horizontal, the impact on the soil surface partially converts the saltator's horizontal momentum gained through wind drag into vertical momentum. This conversion is critical to replenish the vertical momentum dissipated through fluid drag.

The impact of a saltating particle on the soil bed can thus produce a rebounding particle as well as one or more splashed particles.



3.4 Modification of near-surface wind velocity profile

The wind velocity without particles can be described by: $U_{wind,z} = (u^*/\kappa) \ln(z/z_0)$ (3.3)

where $\kappa = 0.40$ is von Kármán's constant, z_0 is the aerodynamic surface roughness, which denotes the height at which the logarithmic profile, when extrapolated to the surface, yields zero wind speed.

The large length scale of the atmospheric boundary layer in which saltation occurs causes the Reynolds number of the flow to be correspondingly large, typically in excess of 10^6 such that the flow in the boundary layer is turbulent. Since the horizontal fluid momentum higher up in the boundary layer exceeds that near the surface, eddies in the turbulent flow on average transport horizontal momentum downward through the fluid. Together with the much smaller contribution due to the viscous shearing of neighboring fluid layers, the resulting downward flux of horizontal momentum constitutes the fluid shear stress. Because the horizontal fluid momentum is transported downward through the fluid until it is dissipated at the surface, the shear stress is approximately constant with height above the surface for flat and homogeneous surfaces.

Equation (3.3) is based on the assumption that the shear stress in the surface layer is constant with height. This is a realistic approximation for flat, homogeneous surfaces, but can be unrealistic for other conditions, such as for surface with non-uniform surface roughness or substantial elevation changes. Furthermore, the drag by saltating particles reduces the horizontal momentum flux carried by the wind.

For small roughness-related Reynolds numbers (< 5), the roughness elements are too small to substantially perturb the viscous sublayer of about 0.4 mm, and the flow is termed aerodynamically smooth. For large roughness-related Reynolds numbers (> 60), the roughness elements are so high that the viscous sublayer is substantially disrupted, and the flow is termed aerodynamically rough and $z_0 = k_s/30$.

Aeolian saltation on Earth takes place for roughness-related Reynolds numbers of 1 to 100 and thus usually occurs in the transition zone between the smooth and rough aerodynamic regimes. Since the roughness in the transition regime does not differ much from that in the aerodynamically rough regime, most studies have used $z_0 = k_s/30$ to approximate the surface roughness.

The near-surface wind profile is modified through momentum transfer to saltating particles. Indeed, it is the retardation of the wind profile through drag by saltating particles that ultimately limits the number of particles that can be saltating under given conditions.

3.5 Saltation to steady state

After the saltation fluid threshold has been exceeded, particles lifted from the surface are quickly accelerated by the wind into ballistic trajectories and, after several hops, can have gathered sufficient momentum to splash surface particles. These newly ejected particles are themselves accelerated by wind and eject more particles when impacting the surface, causing an exponential increase in the horizontal saltation flux in the initial stages of saltation. This rapid increase in the particle concentration produces a corresponding increase in the drag of saltating particles on the fluid, thereby retarding the wind speed. This in turn reduces the speed of saltating particles, such that a steady state is reached when the speed of saltating particles is reduced to a value at which there is a single particle leaving the soil surface for each particle impacting it.

The distance required for saltation to reach steady state is characterized by the saturation length. Its value depends on several length scales in saltation, such as the length of a typical saltation hop, the length needed



to accelerate a particle to the fluid speed, and the length required for the drag by saltating particles to retard the wind speed. The saturation distance is about 10 to 30 m for dry loose sand.

In addition to the saturation length, the adjustment distance is another characteristic length scale over which the horizontal saltation flux increases to a steady state. The corresponding adjustment effect arises because the atmospheric boundary layer flow adjusts to the increased roughness of the surface layer produced by saltation. The increased surface roughness acts as a greater sink of horizontal fluid momentum, which increases the downward flux of fluid momentum, thereby increasing the wind shear velocity for a given free stream wind speed in the atmospheric boundary layer. This process acts as a positive feedback on saltation and is termed the Owen effect. Field studies indicate that the adjustment distance for a flat field site is of the order of about 100 to 200 meters (Davidson-Arnott et al., 2007).

Saltation is in steady state when its primary characteristics, such as the horizontal mass flux and the concentration of saltating particles, are approximately constant with time and distance. Since wind speed can undergo substantial turbulent fluctuations, this is rarely true on timescales longer than minutes or often even seconds, causing saltation to be highly intermittent. In fact, a substantial fraction of sand transport occurs in aeolian streamers or sand snakes, which are probably produced by individual eddies of high-speed air. These streamers have typical widths of about 0.2 meters, thereby producing strong variability on short time and length scales.

The particle concentration in transport-limited saltation is in steady state when there is exactly one particle leaving the soil bed for each particle impacting it. An equivalent constraint is that for each saltating particle lost to the soil bed due to failure to rebound upon impact, another particle must be lifted from the soil bed and brought into saltation by either splash or aerodynamic entrainment.

Wind tunnel experiments show that particles are splashed at impact speeds typical of saltation (about 1 m/s for loose sand). Particle entrainment in steady state is dominated by splash, not by direct fluid lifting.

Figures 3.2 and 3.3 show the saltation distance ($L_{\text{saltation}}$) and saltation height for sand grains in the range of 20 to 500 μm based on the data given in the paper of De Kok et al. (2012). It is assumed that ($L_{\text{saltation}}$) is proportional to the square of the bed-shear velocity. Thus: $L_{\text{saltation}} \sim (u^*)^2$.

The saltation height is: $\delta_{\text{saltation}} \cong 0.04 L_{\text{saltation}}$ and is also shown on the right axis in **Figure 3.2**. The maximum saltation height of 50 μm -grains is about 0.5 m during storm conditions (BF 9).

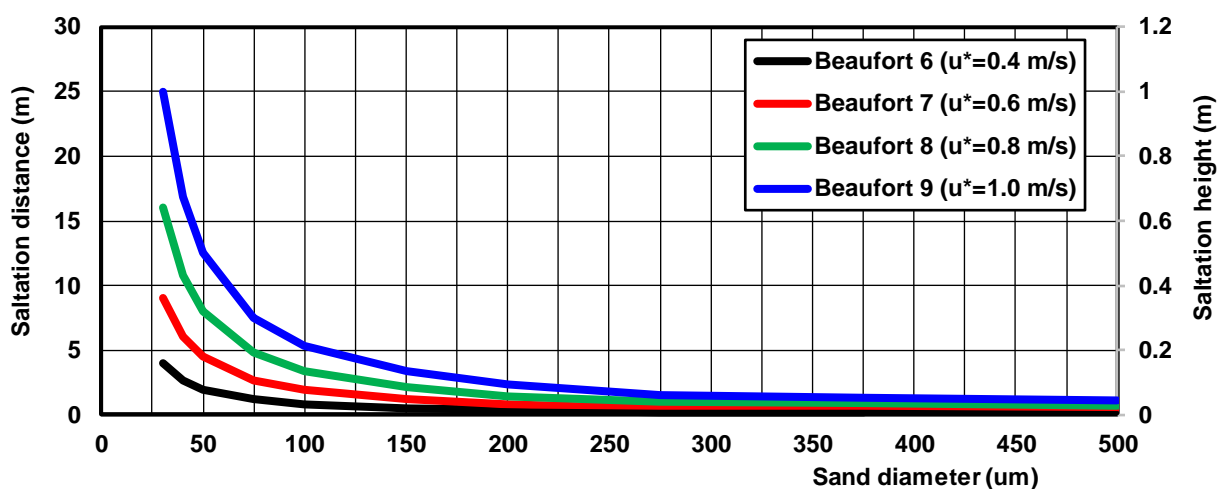


Figure 3.2 Saltation distance as function of sand diameter and wind speed

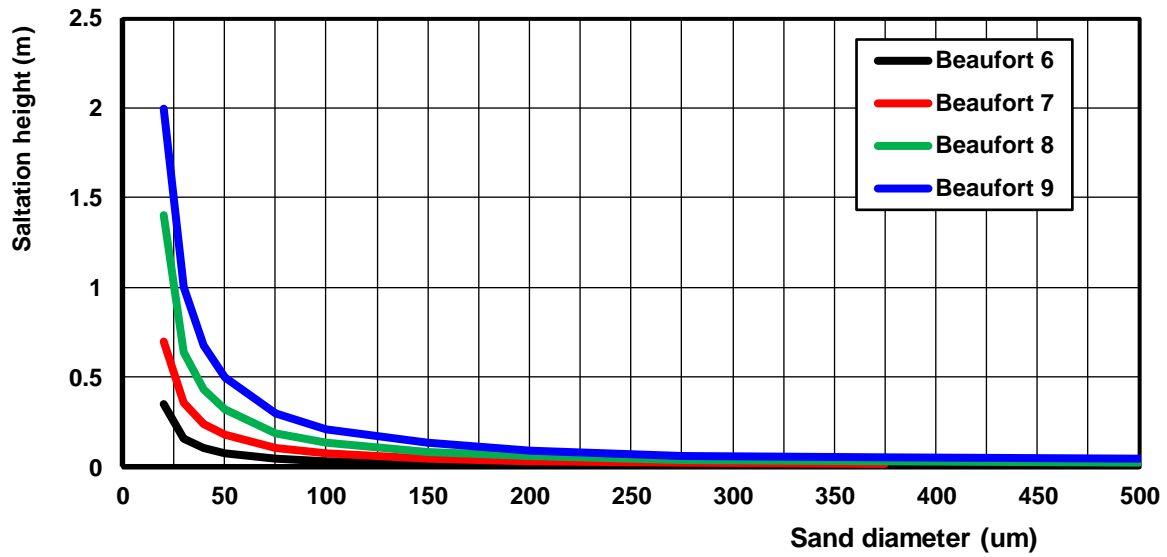


Figure 3.3 Saltation height as function of sand diameter and wind speed

3.6 Saltation mass flux in saturated conditions

The saltation mass flux $q_{s, \text{equilibrium}}$ (in kg/m/s), obtained by vertically integrating the horizontal flux of saltating particles, represents the total sand movement in saltation and is thus a critical measure for wind erosion and dune formation studies. Sediment transport commences as soon as the threshold is exceeded.

Two expressions for dry, loose sand particles are herein given:

$$\text{Modified Bagnold (1941):} \quad q_{s, \text{equilibrium}} = \alpha_B \alpha_{\text{adj}} (d_{50}/d_{50, \text{ref}})^{0.5} (\rho_{\text{air}}/g) [(u^*)^3 - (u^*_{, \text{cr}})^3] \quad (3.4)$$

$$\text{De Kok et al. (2012):} \quad q_{s, \text{equilibrium}} = \alpha_{\text{DK}} \alpha_{\text{adj}} (\rho_{\text{air}}/g) u^*_{, \text{cr}} [(u^*)^2 - (u^*_{, \text{cr}})^2] \quad (3.5)$$

$$\text{Critical shear stress:} \quad u^*_{, \text{cr}} = \alpha_{\text{cr}} \alpha_{\text{mois}} [(\rho_s/\rho_{\text{air}} - 1) g d_{50}]^{0.5} \quad (3.6)$$

$$\text{Shear stress:} \quad u^* = \kappa \alpha_{\text{veg}} \alpha_{\text{sh}} \alpha_{\text{site}} U_{\text{wind}10} / \ln(30h_{\text{wind}}/k_s) \quad (3.7)$$

with:

- $q_{s, \text{equilibrium}}$ = mass flux of sediment at equilibrium conditions (saturated transport);
- d_{50} = particle size (m);
- $d_{50, \text{ref}}$ = reference particle size = $250 \cdot 10^{-6}$ m (250 μm);
- ρ_{air} = density of air ($\cong 1.2$ kg/m³);
- g = acceleration of gravity (m/s²);
- u^* = surface shear velocity due to wind forces (m/s);
- $u^*_{, \text{cr}}$ = surface shear velocity at initiation of motion, threshold shear velocity (m/s);
- k_s = equivalent roughness length scale of Nikuradse (m);
- $U_{\text{wind}10}$ = wind velocity at 10 m above the surface (m/s);
- h_{wind} = height at which wind velocity is defined (= 10 m);
- κ = constant of Von Karman (=0.4);
- α_B = Bagnold factor (= 1.5 to 3 for natural dry, loose sand particles);



- α_{DK} = De Kok factor (= 5 for natural dry, loose sand of 250 μm);
- α_{adj} = adjustment coefficient = $L_{fetch}/L_{adjustment}$; (maximum 1);
- α_{cr} = Bagnold factor for initiation of motion (= 0.11);
- α_{mois} = Moisture coefficient (≥ 1 ; dry sand=1);
- α_{veg} = Vegetation coefficient (none= 1; < 1 if vegetation is present);
- α_{sh} = Sheltering coefficient ($\alpha_{sh} < 1$ for sheltered sites; $\alpha_{sh} = 1$ for exposed sites);
- α_{site} = coefficient for sites higher than the beach (giving higher wind speeds)= $1+0.03h_{site}$;
- h_{site} = site level (crest level) above beach level (m); $h_{site} = 0$ for sand transport at beach.
- L_{fetch} = fetch length at beach (input; about 10 to 100 m normal at beach)
- $L_{adjustment}$ = adjustment length scale of sand transport to equilibrium transport (input; about 100-200 m).

Figure 3.4 shows the windtransport of dry, loose sand based on the formula of Bagnold for three sand diameters. It can be seen that the windtransport increases with grain diameter for wind speeds > 12 m/s (factor $d_{50}^{0.5}$ is dominant) and decreases with grain diameter for wind speeds < 12 m/s (u_{*cr} is dominant). The effect of vegetation is also shown for particles of 300 μm (minor vegetation $\alpha_{veg}=0.75$ or about 5 grass plants per m^2 ; major vegetation $\alpha_{veg}=0.5$ or about 15 grass plants per m^2). Major vegetation strongly reduces the sand transport capacity. The effect of vegetation (marram grass) in combination with 10% moisture is also shown. In conditions with major vegetation and 10% moisture due to rainfall, the sand transport capacity is reduced to almost zero.

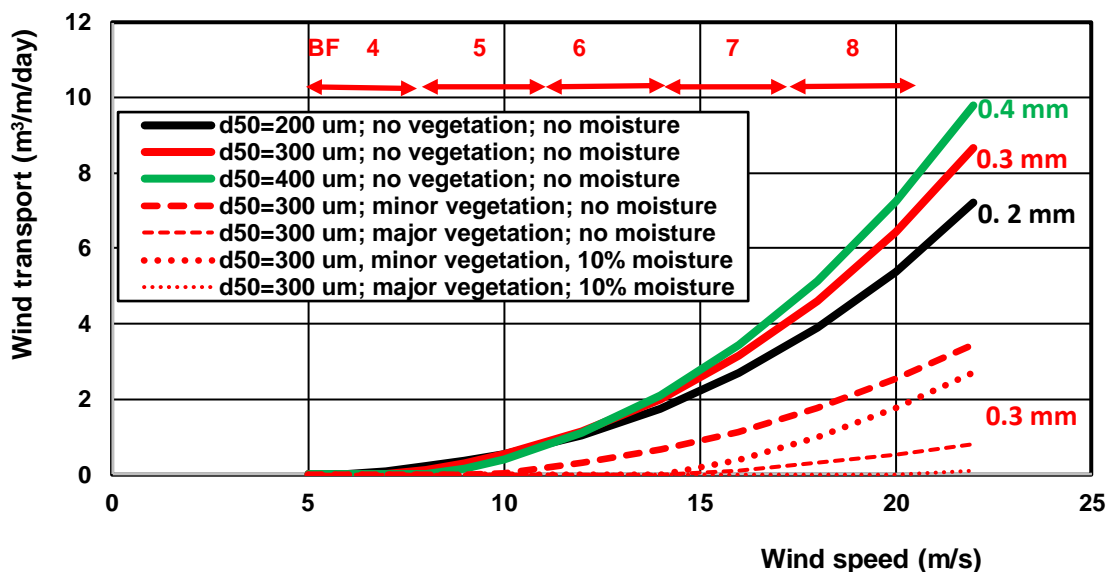


Figure 3.4 Windtransport of dry, loose sand particles at beach based on Bagnold-equation.
($k_s = 0.01$ m, $h_{wind} = 10$ m, $\kappa = 0.4$, $\rho_{air} = 1.2$ kg/m^3 , $\alpha_B = 2$; $L_{fetch} = L_{adjustment} = 100$ m)

Field experiment

A small-scale field experiment was done at the beach of Terschelling (The Netherlands) in July 2013; beach sand of about 0.2 to 0.25 mm (dry, loose particles). A strong wind was blowing parallel to the water line at a wind speed of about $U_{wind10} = 8$ to 10 m/s (Beaufort 5 to 6).

The beach particles were moving by sliding, rolling and saltating in a thin layer of 2 to 3 mm thick with a speed of about 0.1 m/s (carpet-type of transport). About 10% of the surface was moving and wind gusts were very important resulting in intermittent transport processes.

Small-scale ripples were present (height of 0.01 to 0.03 m, length of 0.2 to 0.3 m).



A small trench (length=0.1 m; width=0.1 m) was made normal to the wind. The trench was completely filled in about 30 minutes yielding a transport rate of about $q_s = 0.01 \text{ kg/m/s}$ (bulk density of 1600 kg/m^3).

Using: $d_{50} = 0.225 \text{ mm}$, $k_s = 0.03 \text{ m}$, $U_{wind10} = 9 \text{ m/s}$, yields:

$u_{*,cr} = 0.282 \text{ m/s}$, $u_* = 0.39 \text{ m/s}$ and

$q_{s,bagnold} = 2 \times (0.225/0.3)^{0.5} \times (1.2/9.81) \times [0.39^3 - 0.242^3] = 0.010 \text{ kg/m/s}$

$q_{s,dekoks} = 5 \times (1.2/9.81) \times 0.242 \times [0.39^2 - 0.242^2] = 0.014 \text{ kg/m/s}$

Both values are in good agreement to the measured value of 0.01 kg/m/s .

Example

$d_{50} = 300 \text{ }\mu\text{m} = 0.0003 \text{ m}$; $u_{*,cr} = 0.28 \text{ m/s}$

$u_* = 0.5 \text{ m/s}$: $Q_{s, \text{equilibrium, Bagnold}} = 2 \times (300/300)^{0.5} \times (1.2/9.81) \times (0.5^3 - 0.28^3) = 0.025 \text{ kg/m/s}$

$Q_{s, \text{equilibrium, DEKOK}} = 5 \times (1.2/9.81) \times 0.28 \times (0.5^2 - 0.28^2) = 0.029 \text{ kg/m/s}$

$u_* = 1.0 \text{ m/s}$: $Q_{s, \text{equilibrium, Bagnold}} = 2 \times (300/300)^{0.5} \times (1.2/9.81) \times (1^3 - 0.28^3) = 0.24 \text{ kg/m/s}$

$Q_{s, \text{equilibrium, DEKOK}} = 5 \times (1.2/9.81) \times 0.28 \times (1^2 - 0.28^2) = 0.16 \text{ kg/m/s}$

$u_* = 2.0 \text{ m/s}$: $Q_{s, \text{equilibrium, Bagnold}} = 2 \times (300/300)^{0.5} \times (1.2/9.81) \times (2^3 - 0.28^3) = 1.95 \text{ kg/m/s}$

$Q_{s, \text{equilibrium, DEKOK}} = 5 \times (1.2/9.81) \times 0.28 \times (2^2 - 0.28^2) = 0.67 \text{ kg/m/s}$

3.7 Processes affecting sediment transport

Wind speed acceleration

Wind normal to the beach accelerates along the slope of the foredune and is maximum at the dune crest level.

The influence of topography on wind speed is prominent (Arens et al., 1995). The maximum speed-up increases with height of the foredune. An increase in height from the beach to the dune crest of about 10 m causes an increase in windspeed of about 20% to 40% (see α_{site} -coefficient of Equation 3.7). This will result in an increase of the sand-carrying capacity. A further increase in foredune height $> 10 \text{ m}$ appears to have limited influence, probably because the increase in height (acceleration) is compensated by an increase in roughness due to the presence of irregularities at the dune crest.

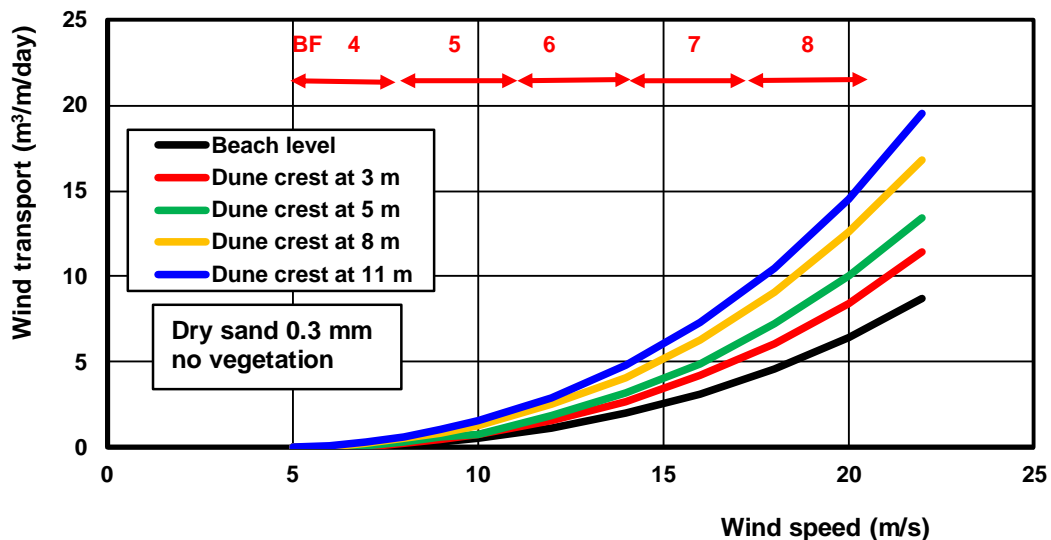


Figure 3.5 Aeolian sand transport at beach level and at various dune crest levels; $d_{50} = 300 \text{ }\mu\text{m}$



Figure 3.5 shows the computed aeolian wind transport at the beach level and at various dune crest levels for sand of 300 μm . The aeolian sand transport increases gradually with increasing crest level as the wind speed increases gradually at higher crest levels due to acceleration effects along the slope of the foredune. The sand transport at a dune crest of 10 m above the beach is about twice (factor of 2) the sand transport at the beach.

Vegetation

Vegetation leads to an increase of the aerodynamic roughness length (z_o), and to an increase of the friction velocity above the vegetation layer. In the vegetation layer itself, momentum is extracted from the air flow and turbulence is produced at the lee side of the roughness elements. The surface friction velocity (u^*) depends on the vegetation physiography, and on the density and spatial configuration of the plants/stems, which can be described by a reduction factor (Equation 3.9; $\alpha_{veg}=1$ for a flat surface without vegetation; $\alpha_{veg} = 0.5$ for plants of 0.1 m high and 5 per m^2 ; $\alpha_{veg} = 0.2$ for plants of 0.2 m high and 15 per m^2).

Shells

Shells (calcium carbonate) can protect the beach surface against erosion of the sand particles. Cadée (1992) has done observations of aeolian transport of large shells (Mya shells) along the Prins Hendrik seadike on the island of Texel (The Netherlands) during and after storm events with wind velocities > Beaufort 10.

His observations are summarized, as follows:

- storm event from South with wind velocities > 30 m/s (BF 12) on 25 January 1990: large quantities of Mya-shells (lengths of 30 to 110 mm; mean length of 60 mm) were transported from the narrow beach on the seaside across the dike and were deposited on the landward side of the dike.
- storm event from Southwest with wind velocities > 30 m/s (BF 12) on 26 February 1990: Mya-shells and other shells were transported over the narrow beach parallel to the dike through saltations with maximum height of 1 m and maximum length of 10 m; shells lying with their hollow side to the beach surface (convex upward) were very stable and hardly movable; shells with their rounded side to the beach (convex downward) were very mobile.
- storm event from South in January 1991 with wind velocities of 24 to 27 m/s (BF 10): Mya-shells were transported across the dike.

Based on this, it can be concluded that shells can only be transported in appreciable quantities during storm events with relatively high wind speeds (BF > 10). The critical wind speed at the onset of motion of large Mya-shells is about 20 m/s (0.75 N/m^2).

Cohesion and rainfall

Cohesion between particles increases surface resistance against erosion (critical shear velocity). Cohesion may result from the presence of moisture, salt, algae, clay, organic matter and carbonate. Moisture contents generally are in the range of 0 to 10%. In situations with a moisture content of 10% (near the water line), the surface is so saturated that aeolian transport reduces to zero even under very strong winds. Small amounts of moisture are characteristic of beach sediments with moisture being created from a variety of sources, including wave uprush, capillary rise from the subsoil water table, wave spray and precipitation (rain fall). Field experiments (Davidson-Arnott, 2007) show that the moisture content at a certain location and thus the critical shear velocity can change over a period of minutes to hours through drainage as the beach water table falls or drying by wind and solar radiation. Surface moisture can limit the rate of release of sediment from the surface, even when sediment transport is continuous, and that it is probably the primary control on the observed adjustment effects on beaches. Even low levels of moisture may effectively reduce the maximum transport rate, i.e. the final transport rate may never reach levels predicted for dry sand.



Based on this, the wind-driven sediment transport is highly variable in space and usually intermittent in time. Moisture increases the resistance of the sand particles against lift and drag, due to cohesive forces of the adsorbed water films surrounding them.

The effects of rainfall on sediment transport by wind are twofold:

1. intensive wind-driven rain can transport sediment by combined splash and saltation processes;
2. residual moisture increases the cohesive forces between particles and therewith the resistance of the sediment against lift and drag.

On sandy beaches, the first process is significant over short time intervals during high-intensity rain events, but this effect is, in terms of quantity, of secondary importance. The second process effect of residual moisture resulting from rainfall lasts over longer time spans and is of crucial importance yielding a significant reduction of critical shear velocity and hence sediment transport (see Equation 3.10; $\alpha_{\text{mois}} > 1$; $\alpha_{\text{mois}} = 1.5$ for surface moisture of 10%; $\alpha_{\text{mois}} = 1.2$ for surface moisture of 3%).

The field work of Davidson-Arnott et al. (2007) at a Canadian beach with sand of 0.26 mm shows large variations of the critical wind speeds: $U_{\text{wind,cr,min}} = 5$ m/s (lowest wind speed with sediment transport) and $U_{\text{wind,cr,max}} = 9$ m/s (highest wind speed without sediment transport) mainly due to variations of the moisture content.

The mean critical wind speed is equal to about $\cong 0.5(U_{\text{wind,cr,min}} + U_{\text{wind,cr,max}})$ and is found to increase with moisture content (about 30% for a moisture content increasing from 0 to 4%).

Davidson-Arnott et al. (2007) have proposed to consider a distribution of threshold values (rather than a single value) with $U_{\text{cr,min}}$ and $U_{\text{cr,max}}$ as the extremes for dry and moist sand (**Figure 3.5**). When the beach is dry, the distribution would probably reflect in some way the particle size distribution. When the beach surface is quite moist the whole distribution will shift towards much higher threshold wind speeds and the shape of the distribution may change to include the influence of cohesion processes. The shape of the distribution for the moist surface should also reflect the potential for surface drying. Incident winds also fluctuate in strength and thus have their own probability distribution, as shown in Figure 3.5. The resulting temporal pattern of sediment entrainment thus reflects the relationship between the two probability curves: one for wind speed and the other for the entrainment threshold. In **Figure 3.5** the threshold distribution for relatively dry sand lies mostly below that of the wind-speed distribution resulting in only a small fraction of time when the speed dropped below the threshold (nearly continuous sediment transport). However, with a relatively moist surface, entrainment will take place only when there is coincidence between higher wind gusts and surface drying shown by the small area of overlap between the two curves on the right-hand side of **Figure 3.5** (only occasional sediment transport).

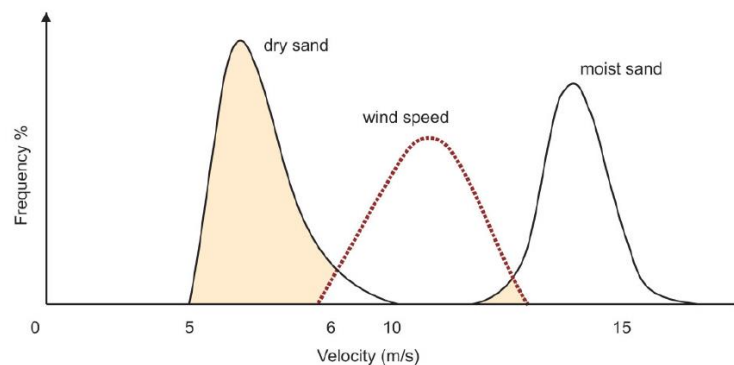


Figure 3.5 Sketch of probability distribution of the critical wind speed for dry and moist sand (Davidson-Arnott et al. 2007)



Adjustment length scale

Transport conditions (u^* and u^*_{cr}) vary in time and space due to variations of environmental parameters. As a result, the actual sediment transport rate will often differ from the equilibrium (potential) transport rate. When transport conditions change, the transport rate adjusts/adapts to the new conditions within a certain time span and within a certain distance. Time and distance are related to each other through the velocity of the saltating grains. Wind tunnel and modelling research on dry, loose sand surfaces has shown that equilibrium transport typically is reached in a few seconds (say 10 s). During saltation, the average horizontal velocity of the grains may be of the order of 3 to 10 m/s. A spatial change in transport conditions may cause changing mass fluxes over a distance of about 10 m for dry, loose sand. The distance over which the sediment transport adjust to new equilibrium conditions is known as the adjustment length scale (L_{ad}) and depends on the particle size and wind speed. The L_{ad} -value is smaller for depositing conditions than for eroding conditions.

The field work of Davidson-Arnott et al. (2007) at a Canadian beach with sand of 0.26 mm shows an adjustment length (the distance at which the transport reaches a maximum) of about 100 to 200 m for the combination of measured wind speeds and moisture contents. The adjustment length associated with each event is defined as the distance along the beach from the upwind boundary, defined by either the vegetation line for offshore-directed winds (from land to sea), or the zone of high moisture content (about 8%) associated with the swash line for onshore-directed winds (from sea to land).

It is not clear whether the maximum transport rate with moist sand is always less than that for dry sand, see **Figure 3.6**. Relatively high transport rates were measured in conditions with offshore winds when sand supplied from the dry upper beach was transported over a damp, hard surface on the lower foreshore. These high transport rates are probably a reflection of the lower momentum losses for sand impacts with the hard surface.

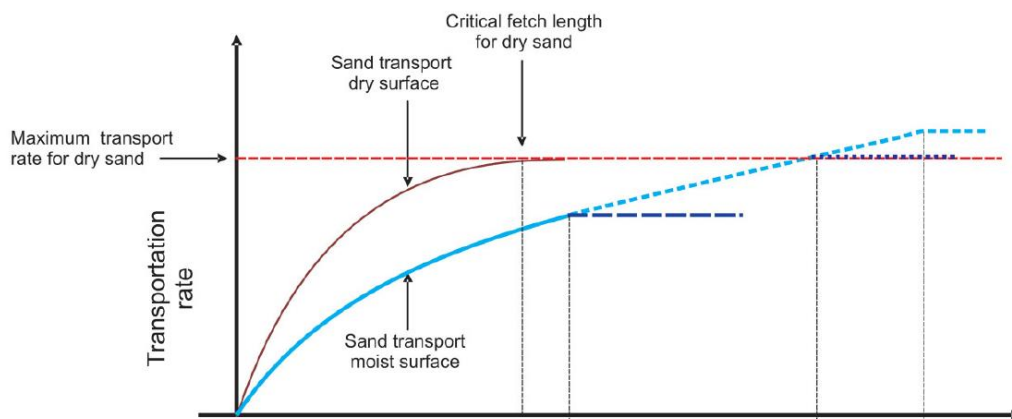


Figure 3.6 Sketch of adjustment length scale for dry and moist sand (Davidson-Arnott et al. 2007)

Where surface moisture is quite high, there is the chance that some saltating grains will adhere to the surface on impact and thus be taken out of the saltation cascade. Where bedforms such as ripples or low barchan dunes are present, grains resting on the surface for more than a few seconds in the lee of the bedform tend to become wet due to capillarity processes and are only dislodged from the stoss slope by impact of saltating grains from upwind. In these conditions it might be expected that the transport rate will never equal that for dry sand. If surface moisture is lower, sufficient dry sand may accumulate where the fetch is long enough (e.g. for highly oblique winds) that the transport rate will eventually equal that for dry sand.

Finally, the transport rate may exceed that for dry sand if the sand supply comes from a dry upwind zone and the sand particles are transported over a moist and hardpacked surface (downwind of the dry surface zone) so that energy loss during collisions with the bed is less than that for a loose, dry sand surface.



The adjustment coefficient can be roughly represented by Equations (3.8) to (3.10).

Modelling of sand transport and sediment transport thus requires not only an ability to predict the wind flow over the sand surface but also, for moist sand, an ability to predict the controls on ejection of grains from the surface and the nature of the rebounds.

Sediment transport in non-saturated conditions

Sediment transport q_s in non-saturated (under-saturated) conditions can be represented as (Van Dijk et al. 1999):

$$q_s = \alpha_{adj} q_{s, equilibrium} \tag{3.8}$$

$$\text{Shear stress: } u_* = \alpha_{veg} \alpha_{sh} K U_{wind10} / \ln(30h_{wind}/k_s) \tag{3.9}$$

$$\text{Critical shear stress: } u_{*,cr} = \alpha_{cr} \alpha_{mois} [(\rho_s/\rho_{air}-1) g d_{50}]^{0.5} \tag{3.10}$$

with:

α_{sh} = sheltering coefficient= 1 for exposed sites; <1 for sheltered sites; =0.8 for beaches under offshore winds;

α_{adj} = adjustment length scale coefficient= $(L_{fetch}/L_{ad})^{0.5}$ with $\alpha_{ad} = 1$ for $L_{fetch} > L_{ad}$;

α_{veg} = vegetation coefficient (< 1); $\alpha_{veg} = 1$ for a flat surface without vegetation;
 $\alpha_{veg} = 0.75$ for plants of 0.1 m high and 5 per m² (minor vegetation);
 $\alpha_{veg} = 0.5$ for plants of 0.2 m high and 15 per m² (major vegetation);

α_{mois} = moisture coefficient (> 1); $\alpha_{mois} = 1$ for a dry, loose sand surface;
 $\alpha_{mois} = 1.2$ for surface moisture of 3%;
 $\alpha_{mois} = 1.5$ for surface moisture of 10%.

L_{fetch} = available fetch length (normal or parallel to shore/dunes/water line);

$L_{adjustment}$ = adjustment length (100 to 200 m).

Sand dunes and ripples

A flat sand bed exposed to a wind strong enough to set grains into motion is unstable. That is, saltation over an initially flat sand bed results in the generation of two kinds of bedforms with distinct length scales: ripples with length scales of up to 1000d₅₀ and dunes, which are typically 5 to 10 meters high but can reach heights of a hundred meters. Dunes occur frequently as isolated objects moving on a firm ground (such as barchan dunes in a corridor) but also as part of compounds evolving on a dense sand bed. Ripples appear most commonly on the surface of dunes as chains of small undulations that orient transversely to the wind trend. The physics governing the formation of ripples and dunes has been studied since the pioneering field works by Bagnold (1941, 1954). Many insights have been gained during the last few decades from computer modeling.



4. Wind-blown sand transport on beaches

Erosive coasts

The primary dune row is continuously eroded and sand is available for aeolian transport in the downwind direction. Sand is blown into the dune field behind the primary dune row which may result in white dunes (sand covering vegetation). Transgressive dunes can be formed moving landwards. Sand dunes are generally highest and without much vegetation along erosive coasts bordering tidal inlets.

Accretive coasts

The supply of sand is so large that a large buffer of sand is present in front of the primary dune row (wide beach plains) resulting in the generation of new embryonal dunes, dune growth and seaward migration of dunes. Vegetation can generally keep up with aeolian transport.

Stabile coasts

New dunes may be generated at the dune toe and in the upper beach zone. Periodic storm erosion by high tides in combination with wind surges can remove the young dunes after which the cycle is repeated. Vegetation can survive as the aeolian transport is not high enough. The height of the primary dune row may grow slowly.

Annual aeolian sand transport along Holland coast

Based on analysis of sounding data, the net annual aeolian transport at the Holland coast between Hoek van Holland and Den Helder (distance of 110 km) is about 2 to 4 m³/m/year in landward direction across the crest of the primary dune row (De Ruig, 1989).

Arens (2009) has studied the effect of beach nourishment on dune growth. About 55 millions m³ of sand (40% in beach zone and 60% in surf zone) was supplied at the Holland coast (Hoek van Holland-Den Helder; 110 km; The Netherlands) between 1997 and 2007. The dune growth volume was found to be about 22% (12 millions m³) of the total beach nourishment volume, which is equivalent with an annual dune volume growth of about 10 m³/m/year.

Example 1

The sand transport equation of Bagnold (1941, 1954) has been used to compute the aeolian transport along a wide beach consisting of dry, loose sand of 0.2 and 0.35mm ($k_s = 0.01$ m, $\rho_s = 2650$ kg/m³, $\alpha_B = 2$, $\alpha_{veg} = 1$, $\alpha_{mois} = 1$, $L_{ad} = 100$ m; $L_{fetch} = 100$ m)

Table 4.1 yields the annual wind transport of sand at a beach with wind from the sectors 180°-210°, 210°-240° en 240°-270° (southwest to northwest). The wind transport (summed over 125 days) is not much affected by particle size.

In practice, the landward transport of sand towards the dune row is a factor of 10 smaller due to moisture and adjustment effects reducing the transport rates (non-saturated transport).

Using: $\alpha_{adj} = 0.55$, $\alpha_{mois} = 1.5$, the windtransport reduces to 13.5 m³/m (normal) and 1.1 m³/m (parallel).



Wind speed (m/s)	Number of days	Wind direction to North	Coast normal to North	Windtransport Bagnold $d_{50}=0.2$ mm (m^3/m)		Windtransport Bagnold $d_{50}=0.35$ mm (m^3/m)	
				normal to shore	parallel to shore	normal to shore	parallel to shore
9 (BF 5)	25	15° (195°)	45°	7.8	-4.5	5.0	-2.9
12 (BF 6)	7	15° (195°)	45°	6.4	-3.7	6.9	-4.0
15 (BF 7)	5	15° (195°)	45°	9.5	-5.5	11.5	-6.6
9	30	45° (225°)	45°	10.8	0	6.9	0
12	10	45° (225°)	45°	10.5	0	11.4	0
15	5	45° (225°)	45°	10.9	0	13.2	0
9	30	75° (255°)	45°	9.4	5.4	6.0	3.5
12	10	75° (255°)	45°	9.1	5.3	9.9	5.7
15	5	75° (255°)	45°	9.5	5.5	11.5	6.6
Totaal	125			84 m³/m	2.5 m³/m	82.4 m³/m	2.3 m³/m

75°=wind direction to which the waves are going; (195°)= wind direction from which the waves are coming

Table 4.1 Windtransport during 125 days of onshore wind

Example 2

A new dune is designed: length= 3 km, width at crest= 40 m; height= 8 m above mean sea level; sand $d_{50}=0.3$ mm; longitudinal dune axis makes an angle of 40 degrees with North (**Figure 4.1**).

The windrose is divided in 4 quadrants (with respect to the longitudinal axis of the dune, see **Figure 4.1**). Each quadrant has 3 sectors of 30°, as follows:

- Quadrant I (SW-NW): sectors 9, 10, 11; total 120 days
- Quadrant II (NW-NE): sectors 12, 1, 2; total 74 days;
- Quadrant III (NE-SE): sectors 3, 4, 5; total 75 days;
- Quadrant IV (SE-SW): sectors 6, 7, 8; total 97 days;
- All quadrants: total 366 days

Computation results based on AEOLIANTRANSPORT.xls (see Table 4.2)

The computed sand transport rates (in $m^3/m/year$) can be summarized, as:

- wind from quadrants I and IV: transport rates are relatively high (dominant);
- wind from quadrant I (120 days)
normal to SE: 35 $m^3/m/year$ for dry sand decreasing to 1 $m^3/m/year$ for wet sand with vegetation;
parallel to NE: 75 $m^3/m/year$ for dry sand decreasing to 1 $m^3/m/year$ for wet sand with vegetation;
- wind from quadrant IV (97 days):
normal to NW: 26 $m^3/m/year$ for dry sand decreasing to 4 $m^3/m/year$ for wet sand with vegetation;
parallel to NE: 110 $m^3/m/year$ for dry sand decreasing to 20 $m^3/m/year$ for wet sand with vegetation;
- wind from quadrants II and III (149 days): relatively small transport values between 10 and 1 normal to crest;
sand transport decreases significantly (factor 5 to 10) due to presence of vegetation;
- sand transport increases/decreases by 10% for smaller grain diameter (0.25 mm) and larger diameter (0.4 mm);
- based on the computed sand transport rates, the erosion of sand at the dune crest (assumed to be covered with vegetation) is estimated to be about 10 to 15 $m^3/m/year$ at the edges of the dune crest, see **Figure 4.2**.

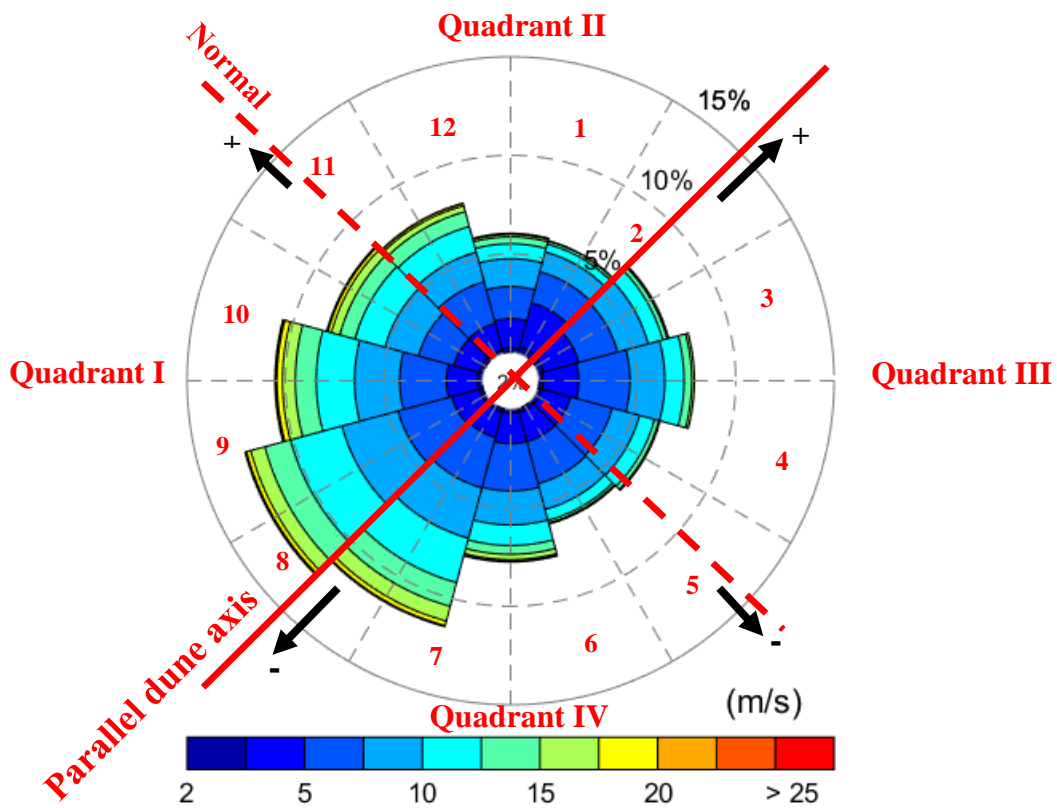


Figure 4.1 Windrose with 4 quadrants and 12 sectors; Sand transport directions (+ or - ;black arrows) Parallel dune axis = red line (angle 40° to North); normal to dune axis= dashed red line

Scenarios	Wind transport (m ³ /m/year including pores)									
	Quadrant I ($\alpha_{sh}=0.8$)		Quadrant II ($\alpha_{sh}=0.8$)		Quadrant III ($\alpha_{sh}=1$)		Quadrant IV ($\alpha_{sh}=1$)		All Quadrants	
	nor mal	paral lel	nor mal	paral lel	nor mal	paral lel	nor mal	paral lel	nor mal	paral lel
Dry loose sand, $d_{50}=0.3$ mm No vegetation ($\alpha_{veg}=1$) No moisture ($\alpha_{mois}=1$)	-35	75	-9	-10	11	-37	26	110	-7	138
Wet sand, $d_{50}=0.3$ mm No vegetation ($\alpha_{veg}=1$) Moisture ($\alpha_{mois}=1.3$)	-6	11	-4	-4	6	-20	17	80	13	67
Dry loose sand, $d_{50}=0.3$ mm Vegetation ($\alpha_{veg}=0.8$) No moisture ($\alpha_{mois}=1$)	-4	7	-2	-2	3	-3	9	40	6	42
Wet sand, $d_{50}=0.3$ mm Vegetation ($\alpha_{veg}=0.8$) Moisture ($\alpha_{mois}=1.3$)	-1	1	0	0	1	-3	4	20	4	18

$\rho_{air}=1.2$ kg/m³; $\rho_{sand}=2650$ kg/m³;

Dry bulk density sand= 1600 kg/m³; adjustment length sandtransport = 100 m; surface roughness $k_s=0.01$ m

α_{veg} = vegetation coefficient; α_{mois} = moisture coefficient; α_{sh} = sheltering coefficient (reduced wind)

Normal: - = sand transport normal to dune crest in direction south-east; + = in direction north-west

Parallel: - = sand transport parallel to dune crest in direction south-west; + = in direction north-east

Table 4.2 Windtransport at sand dune

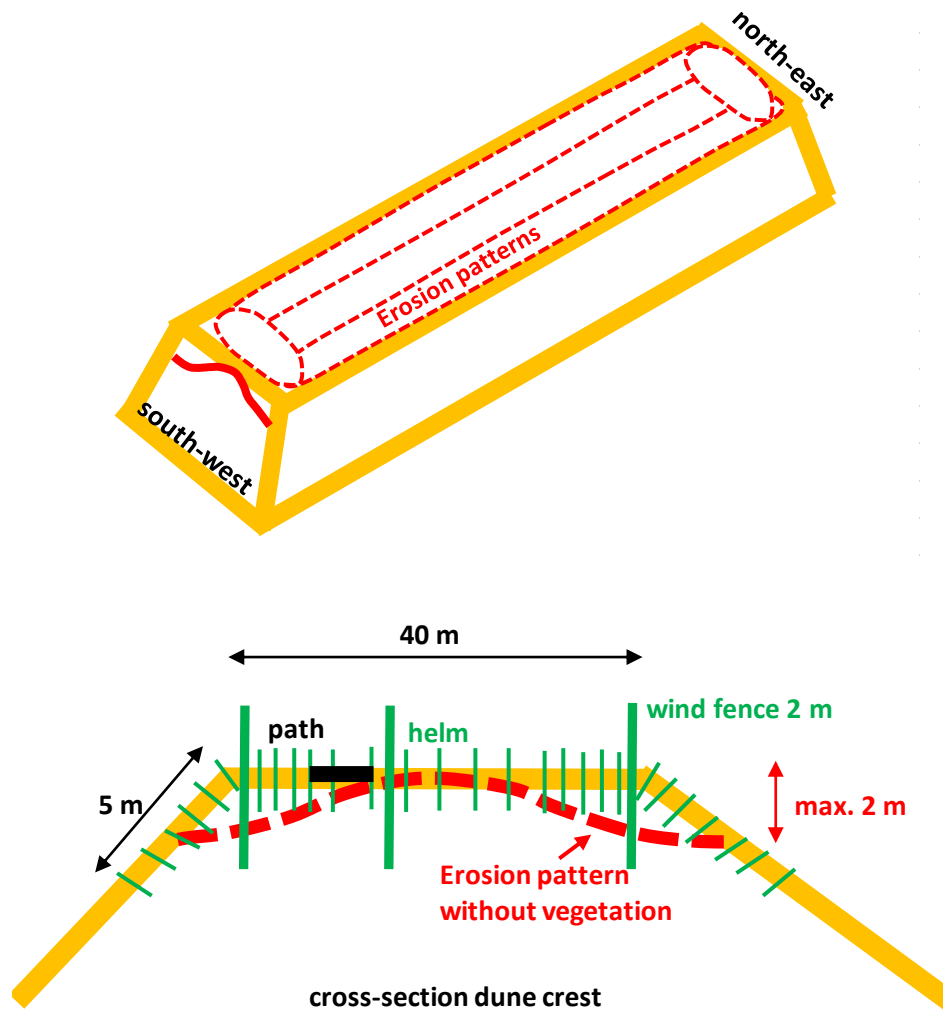


Figure 4.2 Wind erosion at dune crest and preventive measures (vegetation and wind fences)

5. Preventive measures to reduce erosion

Erosion due to wind can be reduced to less than $5 \text{ m}^3/\text{m}/\text{year}$ by taking the following measures:

- grass-type vegetation (spinifex; 9 to 10 plants per m^2);
- temporary wind screens/fences (brushwood; lengths of 2 to 2.5 m);
- paper pulp can be sprayed (thin layer) on dry loose sand to reduce erosion (temporary) at dune surfaces without vegetation.

The most effective measure is to plant grass-type vegetation. Usually, it is sufficient to use about 10 plants per m^2 . The plants are manually pushed into small holes made in the dry sand. A team of 5 to 10 men can make a production of about 5000 m^2 per day. Machinery (tractors) can be used at flat surfaces. Planting is done in seasons with some rain, as the plants need some water for growth. After a few years the root system of the plants is penetrated into the sand body over a length of 1 to 3 m.



6. References

- Arens, 2009.** Effecten van suppleties op duinontwikkeling. Rapport 2009.02, Amsterdam
- Arens, S.M., Van kaam-Peters, H.M.E. and Van Boxel, J.H., 1995.** Air flow over foredunes and implications for sand transport. *Earth Surface Processes and Landforms*, Vol. 20, 315-332
- Bagnold, R.A. 1941, 1954.** The physics of blown sand and desert dunes. Methuen, New York.
- Cadée, G. 1992.** Eolian transport of Mya shells, *Palaios*, Vol. 7.
- Davidson-Arnott, R.G.D. et al., 2007.** The effects of surface moisture on aeolian sediment transport threshold and mass flux on a beach. *Earth Surf. process. Land forms*.
- De Kok, J.F. et al., 2012.** The physics of wind-blown sand and dust. *Rep. prog. Phys.* Vol. 75, 106901.
- De Ruig, J.H.M., 1989.** De sediment balans van de Hollandse kust 1963-1986. Rapport GWAO-89.016 Dienst Getijdewateren, Rijkswaterstaat, Den Haag
- Van Dijk, P. M. et al. 1996.** The influence of rainfall on transport of beach sand by wind. *Earth Surface Processes and Landforms*, Vol. 21, 341-352.
- Van Dijk, P.M. et al. 1999.** Aeolian processes across transverse dunes, part II. Modelling the sediment transport and profile development. *Earth Surf. Process. Landforms*. Vol. 24, 319-333